WIND TUNNEL THREE-DEGREE-OF-FREEDOM DYNAMIC RIG FOR CONTROL VALIDATION

**Dmitry I. Ignatyev *†, Maria E. Sidoryuk*, Konstantin A. Kolinko*,
and Alexander N. Khrabrov***
* Central Aerohydrodynamic Institute named after N.E. Zhukovsky, Zhukovsky, Russia
† Moscow Institute of Physics and Technology, Zhukovsky, Russia

Abstract

High-angles-of-attack dynamics of modern aircraft is complicated with hazardous phenomena such as wing rock and stalling. Autonomous dynamically scaled aircraft mock-up mounted on three degree of freedom dynamic rig is proposed for studying the high-angle-of-attack behavior and control law testing. To stabilize the mock-up at high angles of attack two controllers are designed, namely, using the robust and model reference adaptive control techniques. Wind tunnel experiments using the proposed equipment show that both controllers ensure stability of the aircraft mock-up at high angles of attack.

1 Introduction

Significant extension of the angles-of-attack range used in the modern flight leads to necessity of more adequate modeling of aircraft dynamics. At high angles of attack the aerodynamics becomes significantly nonlinear and depends on the prehistory of motion [1 - 3]. This is why the wind tunnel studies of the unsteady aerodynamic characteristics and dynamics at high angles of attack should be carried out using motions, which are close to natural controllable aircraft maneuvers as much as possible. Such maneuvers can be implemented using dynamic rigs with various degree-of-freedom (DOF) motions.

Single degree-of-freedom rigs are widely used for investigations of unsteady aerodynamics and nonlinear dynamics. The most of the facilities provide free-to-roll or free-to-pitch motions [4 – 7]. In [5] an aircraft model is mounted on a tail sting of the free-to-roll dynamic rig equipped with a single DOF gimbals. The development of self-induced oscillations in roll can be studied using this rig. The rig of free-to-pitch oscillations [5] is used to investigate unsteady longitudinal aerodynamic characteristics. A model trimming incidence is specified with deflection angles of longitudinal control surfaces. If the specified trimming incidence is in the angle-of-attack range where the positive damping is observed the pitch self-induced oscillations can develop in the experiment [6].

Model motions that are close to the natural aircraft maneuvers can be implemented using a dynamic rig with 3 or more degrees-of-freedom. A study using the 3DOF actively controlled dynamically scaled aircraft model and gimbals were reported in [8]. A model was mounted on the under-fuselage vertical support strut that was fixed to the floor in a low subsonic wind tunnel. 4DOF dynamic rig was also discussed in [9]. The aircraft model was suspended on a stiff vertical rod that passes through a 3DOF gimbals mechanism within the model. It was shown that using the kinematic configurations mentioned above the investigation of unsteady aerodynamic characteristics could be fulfilled only in a restricted range of small and moderate angles of attack. A maneuver rig [10] is proposed for the investigation of 5 DOF motions and can be used for high-angle-of-attack maneuvers. The testing aircraft models in studies presented in Refs. [8-10] are equipped with digital servos, which enable motions of the control surfaces, and data acquisition systems, which gather information about the model

attitudes. Usage of micro electromechanical systems (MEMS) sensors [10] helps to improve the accuracy of the experiment. The discussed multi-degree-of-freedom rigs were used for investigation of the aircraft instability regions and identification of unsteady aerodynamic characteristics.

In the present study 3DOF dynamic rig is considered not only for investigation of critical flight regimes but also for control law testing. The rig is designed with a dorsal support strut oriented along the wind tunnel flow to increase the angle-of-attack range [11]. Hereby, the limitations due to the under-fuselage support and vertical rod are removed, and high angles of attack region can be studied [12]. The proposed 3-DOF rig design allows investigation of large angles of attack phenomena, such as longitudinal pitching limit-cycle oscillations, or lateral–directional phenomena, such as wing rock and stalling [13]. The other advantage of the developed experimental facility is the usage of an on-board computer for acquisition, handling of the flight data and, simultaneously, for operation of the model control algorithms. Such design enables the model to be autonomous during the experiments and the control laws to be tested in a semi-free flight.

In addition, current work is focused on the designing of algorithms that stabilize the scaled aircraft mock-up at high angles of attack. The main interest is connected with testing them using the autonomous model mounted in the 3DOF gimbals. The robust synthesis technique is considered for designing of the proportional controller, which ensures stability of the tested mock-up within the wide range of experiment parameters. At the same time, the standard Model Reference Adaptive Control (MRAC) approach, which is usually used for dealing with model uncertainties, is applied. The experimental results of testing the designed controllers are presented in the paper.

2 Wind Tunnel Test Facility

A schematic view of a dynamic rig in wind tunnel (sting located along the velocity of the flow) is shown in Fig. 1. 3-DOF gimbals are used to achieve the rotation in three degrees of freedom: pitch, roll, and yaw. The dynamic rig is designed to be installed in the open working section of the TsAGI wind tunnel T-103 of low subsonic velocities.

In addition to 3DOF motion, any single-DOF configuration and any 2DOF motion combination can be modelled.

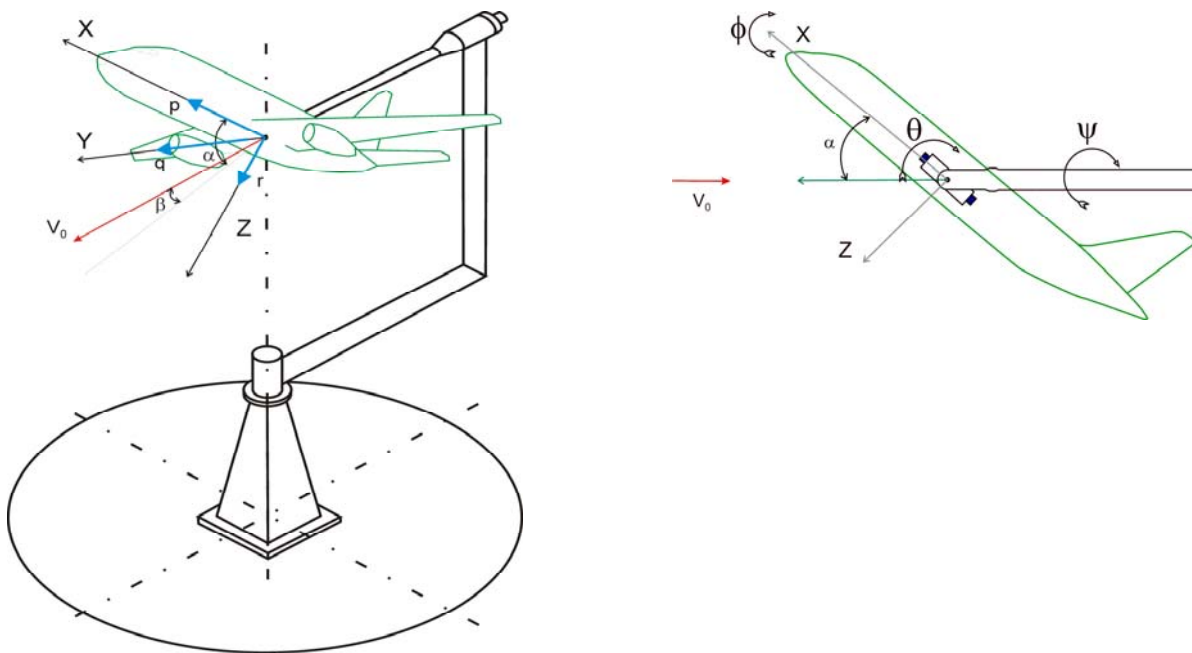The mock-up is a dynamically scaled model

Fig. 1. The Dynamic Rig For Aircraft Dynamics Simulation And Control Clearance

of an aircraft with low aspect ratio sweep wing, which wing span is about 1 m and the mass is about 4.5 kg. It has a conventional set of control surfaces driven by servos: differential stabilator, ailerons, and a rudder. The attitudes of the model in gimbals are measured by three high resolution optical encoders (accuracy ±0.07 deg). An inertial measurement unit (IMU) is used also for measurement of angular velocities with accuracy ±0.025 deg/s. The mock-up is equipped with the on-board computer, which is used for data acquisition and handling, operation of the control algorithms, and connection with a computer "ground station" via the Bluetooth wireless link. Before starting the experiment the tested control law is uploaded on the on-board computer. The computer "ground station" is used for monitoring and controlling of the model during the experiments. Data acquisition is performed at frequency 100 Hz, and control is performed at 50Hz. Figure 2 gives a view of the on-board computer with IMU, as well as 3DOF gimbals.
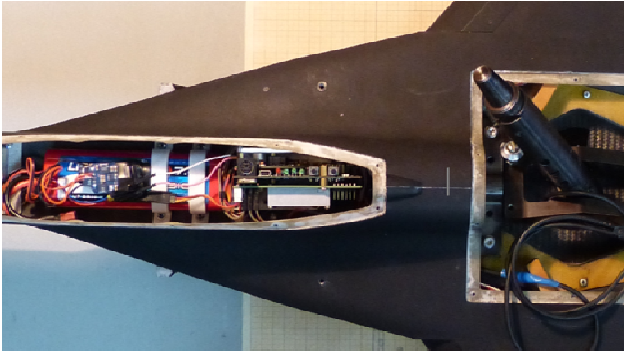

Fig. 2. The on-board computer with IMU, and 3DOF gimbals

3 Mathematical model

A mathematical model of dynamics of the mock-up on the test rig in the wind tunnel was developed for designing of the experiments [11, 12, 13]. Position of the aircraft model in the 3DOF gimbals is defined by three rotational angles ψ, θ, ϕ (Fig. 1). The dorsal holder allows free rotation in yaw ψ. The pitch angle θ can be varied inside the interval [20, 120] degrees, and roll angle ϕ lies in the range [-40, 40] degrees. The dynamics in the 3DOF gimbals is

described by the following system of differential equations [11]:

$$\dot{\theta} = -r\sin\phi + q\cos\phi,$$
$$\dot{\psi} = (r\cos\phi + q\sin\phi)/\sin\theta,$$
$$\dot{\phi} = p - (r\cos\phi + q\sin\phi)/\mathrm{tg}\theta, \quad (1)$$
$$\dot{\omega} = \mathbf{J}^{-1}(-\omega \times \mathbf{J}\omega + \mathbf{M}(\alpha, \beta, \omega, \delta)).$$

where $\omega = (p, q, r)^T$ is a vector of body-axis angular velocity components of the model, $\delta = (\delta_e, \Delta\delta_e, \delta_a, \delta_r)^T$ is a control vector consisting of the mean stabilator δ_e (elevator), the differential stabilator $\Delta\delta_e$, the aileron δ_a, and the rudder δ_r surface deflections. $\mathbf{M} = (M_a, M_g, M_f)^T$ is the vector of the aerodynamic, gravity, and gimbals friction moments, respectively. Angle of attack α and sideslip angle β are defined by the following relations:

$$\tan\alpha = \tan\theta\cos\phi,$$
$$\sin\beta = \sin\theta\sin\phi.$$

Body-axis components of the non-dimensional aerodynamic moment can be expressed through the following form:

$$C_m = C_{m0}(\alpha, \delta_e) + C_{mq}(\alpha)q$$
$$C_l = C_{l0}(\alpha, \beta) + C_{lp}(\alpha)p + C_{lr}(\alpha)r + \Delta C_{l\delta_r}(\alpha, \delta_r, \delta_a, \delta_e, \Delta\delta_e)$$
$$C_n = C_{n0}(\alpha, \beta) + C_{np}(\alpha)p + C_{nr}(\alpha)r + \Delta C_{l\delta_r}(\alpha, \delta_r, \delta_a, \delta_e, \Delta\delta_e)$$

The dependence of roll and yaw moment coefficients on sideslip angle and angle of attack are presented in Fig. 3. At the angles of attack higher than 10 deg the aerodynamic coefficients become strongly nonlinear. At the same time due to aerodynamic shadowing of the control surfaces the control efficiency is strongly degraded [13]. The more detailed data on the aerodynamic, gravity, and gimbals friction moments can be found in [12, 13].
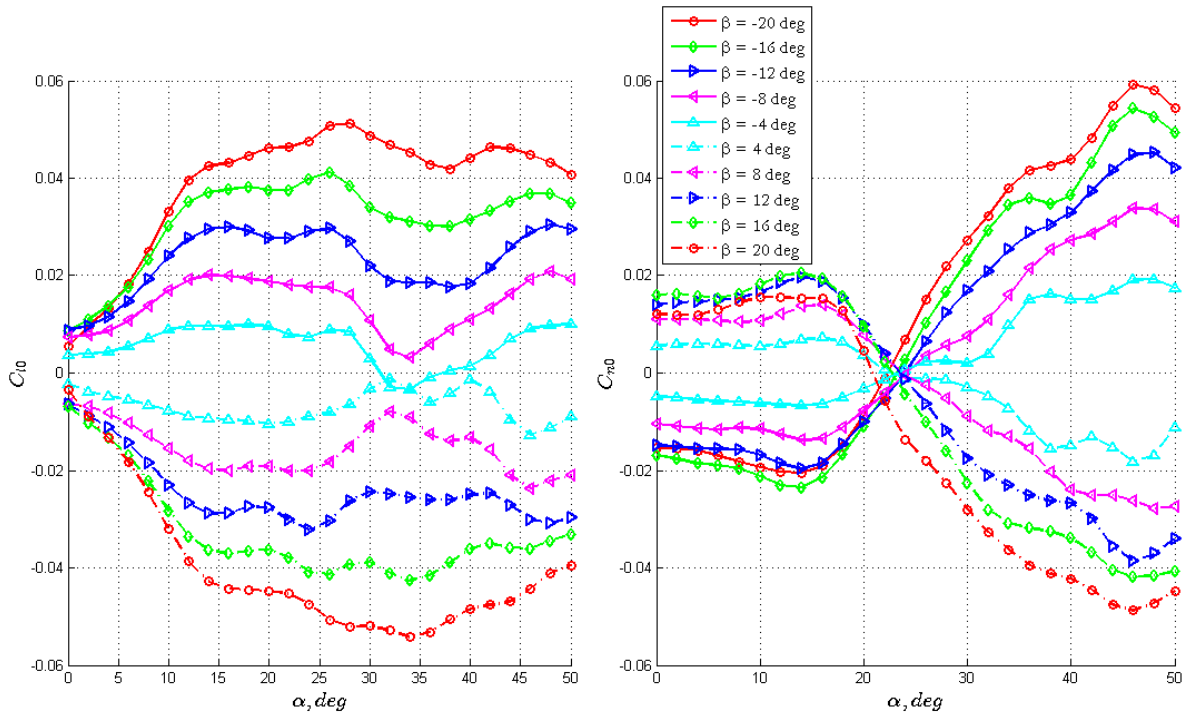
Fig. 3. Influence of sideslip on roll and yaw moments.

In order to justify the possibility of studying the dynamics of the aircraft at high angles of attack in the wind tunnel using the scaled mock-up mounted on the 3DOF gimbals, the comparison of computer simulations of the mock-up wind tunnel dynamics and the free-flying dynamics was carried out in [12]. The model of aerodynamics that is used for the simulations of the wind tunnel experiments is augmented with the model of forces acting on the scaled aircraft mock-up and is used for the free flight simulations. The scales of the aircraft mock-ups are considered the same. Results of the numerical simulation of wing rock motion in the 3 DOF gimbals in wind tunnel shows that the amplitudes and frequencies of self-induced oscillations in angles of attack and sideslip, as well as the angular rates, obtained for the wind tunnel and for the free flying model are rather close [13].

Comparison of the eigenvalues of the free model motion in the vicinity of horizontal flight and in 3DOF gimbals shows that they are close. For example, at α=35 deg, the eigenvalues of spartial short period mode equal to 0.2282±0.5911, -0.4072±0.6654 i, -2.111, and for the system of order 6 in motion in 3DOF gimbal they are 0.2682±0.5687, -0.4025±0.5749

i, -2.187, 0, respectively. Trimmed values of the stabilator deflection for the wind tunnel (WT) model and for the free-flying (FF) models are close to each other $\delta_{e_{trim}}^{WT}$ =-19.7 deg, and $\delta_{e_{trim}}^{FF}$ =-17.9 deg. These results demonstrate the similarity of dynamics of the aircraft model mounted on the 3DOF gimbals in the wind tunnel and the free-flying aircraft model of the same scale. Thus 3DOF gimbals technique can be used for studying of the phenomena of nonlinear aircraft dynamics observed at high angles of attack such as wing rock, stall, and spin.

5 Control Law Design

The available experimental setup allows testing of different control laws that provide stability of the aircraft model at high angles of attack, suppressing self-oscillations and preventing stalling. In this study two control laws are to be validated using the designed facility. The first of these is the most simple proportional control law. It is designed using the robust synthesis technique [14, 15]. The second one is a proportional controller augmented with a model reference adaptive control [16].

4.1 Robust Control Law

The proportional control law for improving lateral/directional stability and suppressing wing-rock and stalling have the following form:

$$\boldsymbol{\delta}_{prop} = \mathbf{K} \cdot \mathbf{x} \qquad (2)$$

where $\boldsymbol{\delta}_{prop} = [\Delta\delta_e, \delta_r, \delta_a]^T$ is the vector of control effectors, namely, differential stabilator, rudder and aileron, $\mathbf{x} = [\phi, \psi, p, r]^T$ is the state vector of the lateral/directional variables, and $\mathbf{K}$ is the control gain matrix. Angles ϕ and ψ, which are used for feedback, are measured by encoders, and angular rates are measured by IMU. The control law gains were calculated using the multi-model/multi-objective state-feedback synthesis with pole placement in LMI regions [14]. This approach allows the robust controllers for a certain range of parameters of parameter dependent plants to be obtained. For the plant specified by state-space equations

$$\dot{x} = A(t)x + B_1(t)w + B_2 u(t)$$
$$z_\infty = C_1(t)x + D_{11}(t)w + D_{12}u(t)$$
$$z_2 = C_2(t)x + D_{22}(t)u$$

the method allows to compute the state-feedback control $\boldsymbol{\delta}_{prop} = \mathbf{K} \cdot \mathbf{x}$ that keeps the H_∞ norm of the closed-loop transfer function from the disturbance w to the error z_∞ and H_2 norm of the closed-loop transfer function from the disturbance from w to z_2 below some prescribed values, and places the closed-loop poles in the LMI region. The matrices $A(t), B_1(t), B_2(t), C_1(t), D_{11}(t), D_{12}, C_2(t), D_{22}(t)$ depend on the flight regimes. The control law guarantying the closed-loop stability with desirable response and transient behavior for all flight regimes can be synthesized using this technique.

In the present design of lateral/directional control law the range of angles of attack varies from 20 deg up to 45 deg which corresponds to trimming values of elevator deflections from -12 up to -28 degrees. The pole placement region was chosen in the intersection of the half-plane x<-1.2 and the conic sector centered at the origin and with inner angle $3\pi/4$. The design objective was to minimize the H_2 norm of the vector $[\phi, \psi, p, r]^T$ as well as the control efforts (with weights) in the presence of the disturbances, including the turbulence. The result of the control design procedure is the control law of the form (5). The designed gain matrix is the following

$$\mathbf{K} = \begin{bmatrix} 0.0 & 1.0 & 0.1 & 0.1 \\ 1.0 & -1.8 & -0.2 & -1.2 \\ -0.6 & 2.0 & 0.2 & 0.75 \end{bmatrix} \qquad (3)$$

To improve longitudinal stability and suppress pitch oscillations, a simple pitch damper is used to produce the following control input on elevator deflection

$$\delta_e = \delta_{e\,trim} + K_q q \qquad (4)$$

with $K_q = 0.4$.

Before the wind tunnel experiments the control law (2)-(4) was tested through a nonlinear simulation of discrete-continuous system, where the dynamical system is continuous, and the controller is discrete. The resulting system consists of the equations of motion of the aircraft mock-up mounted on the gimbals (1), the control law (2)-(4). The system dynamics was augmented with the wind tunnel turbulence. The system time delay τ=0.04s is introduced in the model. The controller discrete time is dt=0.02 sec, which is similar to the signal update time of the aircraft mock-up servos. The dynamics, limitations of angles and rates of servos are also included in the model. The simulation results for various elevator deflections are given in Fig. 5. The elevator deflections correspond to high-angle-of-attack region, where the lateral-directional instability of the open-loop system occurs. Control law is switched on at t=2 s. Before the control switch-on the system demonstrates dangerous rotation in yaw and roll with high rates, accompanied with oscillations in pitch. One can see that the designed controller ensure stability of the system. The observed parasitic small amplitude oscillations are due to the wind tunnel turbulence.
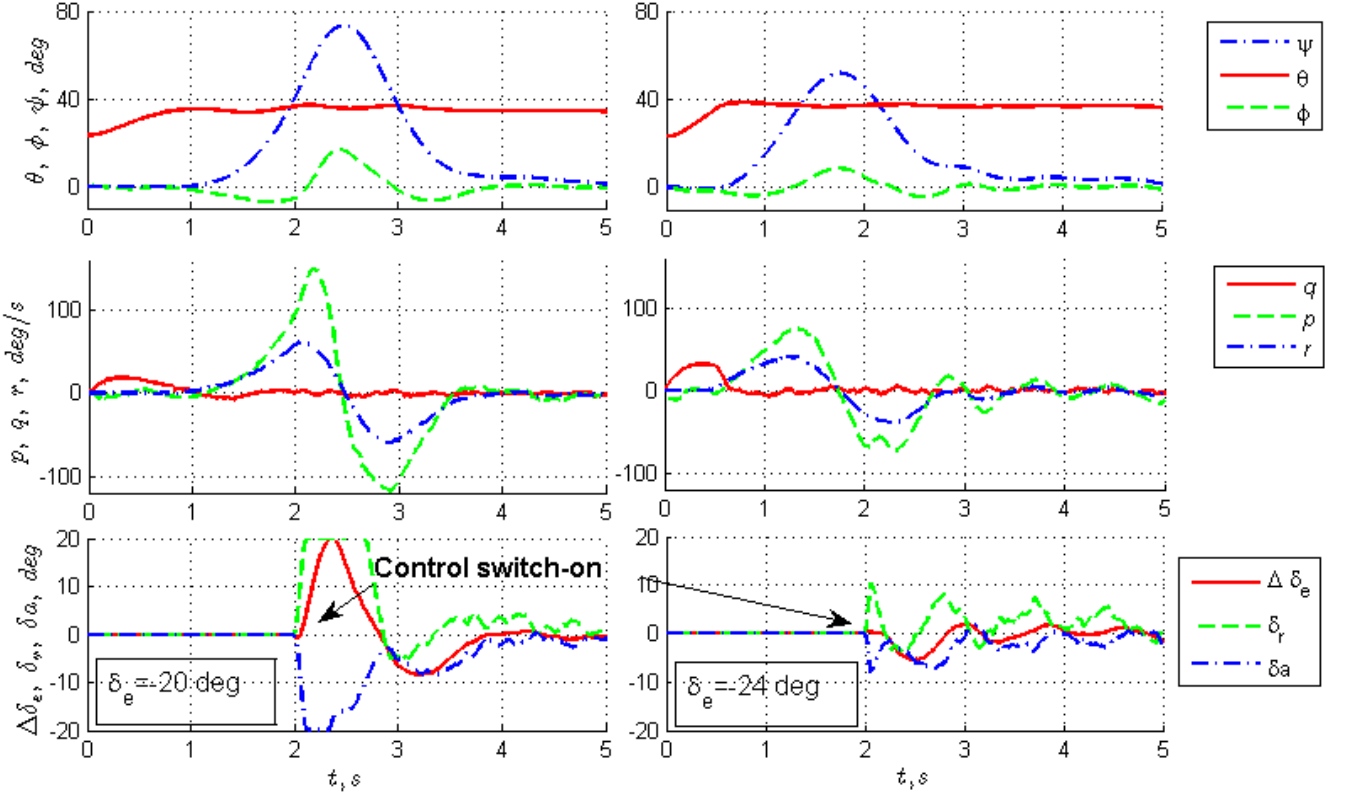
Fig. 5. Loss of stability and recovery using the proportional controller at t=2s.

4.2 Neural Network Adaptive Control

In this section an adaptive control law stabilizing model in the entire attainable angle-of-attack range is discussed. The standard Model Reference Adaptive Control (MRAC) [16, 17, 18] is used.

The proportional control law $\boldsymbol{\delta}_{prop}$ (2) is augmented with the adaptive one

$$\boldsymbol{\delta} = \boldsymbol{\delta}_{prop}(t) - \boldsymbol{\delta}_{adapt}(t), \qquad (5)$$

where the adaptive controller $\boldsymbol{\delta}_{adapt}(t)$ is specified by the following equation

$$\boldsymbol{\delta}_{adapt} = \tilde{\mathbf{W}}^{T}(t) \cdot \boldsymbol{\beta}(x(t)), \qquad (6)$$

where $\boldsymbol{\beta}: R^{n} \to R^{s}$ is a vector of basis functions $\boldsymbol{\beta} = [\beta_1(\mathbf{x})\beta_2(\mathbf{x})...\beta_s(\mathbf{x})]^{T} \in R^{s}$, $\tilde{\mathbf{W}} \in R^{s \times m}$ is the matrix of weights. The weight update law is the following:

$$\dot{\tilde{\mathbf{W}}} = -\Gamma \mathbf{e}^{T} \mathbf{P} \mathbf{B} \boldsymbol{\beta}(x) - \sigma \tilde{\mathbf{W}}(t), \qquad (7)$$

where $\Gamma > 0$ is an adaptation gain, $\mathbf{e} = (e_1,...,e_n)^{T}$, $e_i = x_i - x_{mi}$ is the state tracking error. $\mathbf{P} \in R^{n \times n}$ is the positive–define solution of the Lyapunov equation for the reference system, which dynamics is specified by the matrix $\mathbf{A}_{m}$

$$\mathbf{A}_{m}^{T}\mathbf{P} + \mathbf{P}\mathbf{A}_{m} = -\mathbf{Q}, \quad \mathbf{Q} = \mathbf{Q}^{T} > 0.$$

The nonlinear parameterization of the adaptive control law via introducing the modification term $\sigma\tilde{\mathbf{W}}(t)$, where $\sigma > 0$, is used to improve the stability [19]. The proof of stability using the Lyapunov function can be found in [17].

While synthesizing the control law stabilizing the wind tunnel model the following parameters are used. The Gaussian Radial Basis Functions (RBF) are used in (6)

$$\beta_i(x) = \exp[-\|x - c_i\|^2 / (d_i^2)], \quad i = 1,...,s,$$

where $\|\cdot\|$ denotes the Euclidian norm, and c_i and $d_i > 0$ are the center and widths of the ith

kernel function, respectively. We use the state vector containing 6 components $\mathbf{x} = (\theta, \psi, \phi, q, r, p)^T$. Single dimension basis functions are used, namely,

$$\beta_{ki} = \exp\left(\frac{-(x_k - c_{ki})^2}{d_k^2}\right),$$

where each set $\beta_{ki}, i = 1..l$ corresponds to each component of the state vector x_k. For each component x_k of the input domain consisting of l=21 centers are used, and these results in $21 \times 6 = 126$ total number of RBF centers. The centers $c_{ki}, i = 1..n$ are uniformly spaced in k dimension and cover all variation range of the corresponding component x_k. Single dimension basis function are used because it is difficult to guarantee persistency of excitation for high dimension of the RBF input space [20].

For proper overlapping between the kernel functions the width is adjusted according to the following rule [18]

$$d_k = \frac{x_{k\max} - x_{k\min}}{2(\sqrt{l} - 1)},$$

where $x_{k\max}$, $x_{k\min}$ are the expected maximum and minimum values of the component of the state vector. The gains in (7) were the following Γ=30, $\sigma = 1$.

It should be noted that according to (5) the proportional law is augmented with the adaptive RBF controller. The current architecture is reasoned by the following considerations. The obtained information about the aircraft aerodynamics is used to design the proportional control law in the optimal way using the robust technique, and the uncertainties of the available information are matched with the adaptive controller.

The simulation results obtained for different stabilizer deflection $\delta_e = -20$ deg and $\delta_e = -24$ deg are shown in Fig. 6. The plots show that the proposed adaptive control stabilizes the model, suppresses the self-induced oscillations and prevents stall.
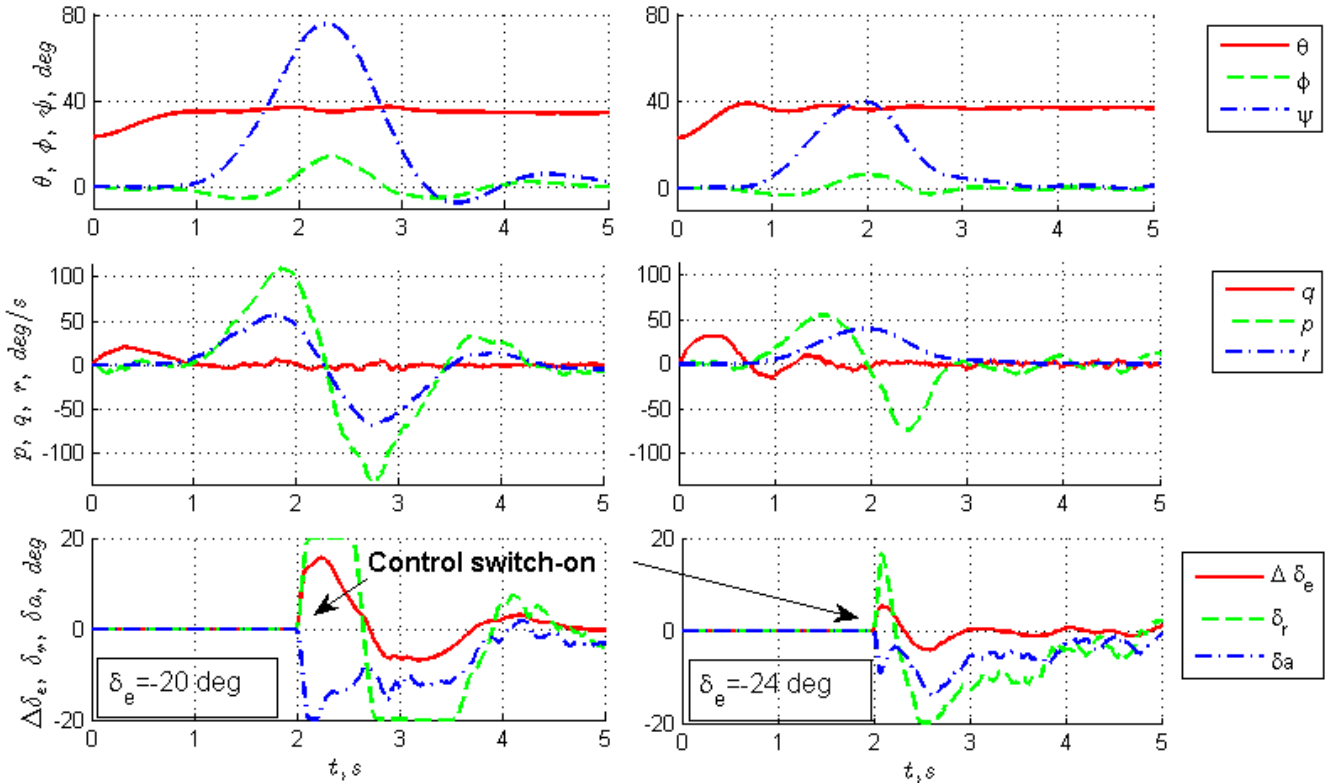

Fig. 6. Loss of stability and recovery using the adaptive controller at t=2s.

5 Testing of Control Algorithms

The experimental results obtained using the 3DOF gimbals are presented in this section. At the beginning the open-loop system dynamics is investigated. The elevator is successively increased in the step-wise manner from $\delta_e = -12$ deg up to $\delta_e = -28$ deg with the step $\Delta\delta_e = -2$ deg that leads to successive step-wise nose-up motion. The responses of the system are shown in Fig. 7.

One can see that at small angles of attack the model exhibits stable dynamics with nonzero angles of roll and yaw. At the stabilator deflection $\delta_e \leq -20$ deg the model high-angles-of-attack departure ($\alpha > 30$ deg) is observed and the open-loop system becomes unstable. Rotation of the model with respect to velocity vector, accompanied with high amplitude self-induced oscillations in roll and pitch is

observed. Thus the region of instability for this aircraft model is observed at angles of attack higher than 30 deg.

The designed control laws are experimentally tested in the wind tunnel using the autonomous mock-up mounted on 3DOF gimbals. In addition fine tuning of the control parameters are carried out.

The MRAC controller is compared with the open-loop dynamics in the Fig. 7. One can see that the proposed control law ensures stability of the system in the considered range of parameters.

The responses for the proportional and the adaptive controllers obtained in the experiments are presented in the Fig. 8. The figure demonstrates that both controllers prevent stalling and wing rock of the mock-up. The residual oscillations observed on the figures are due to the wind tunnel turbulence.
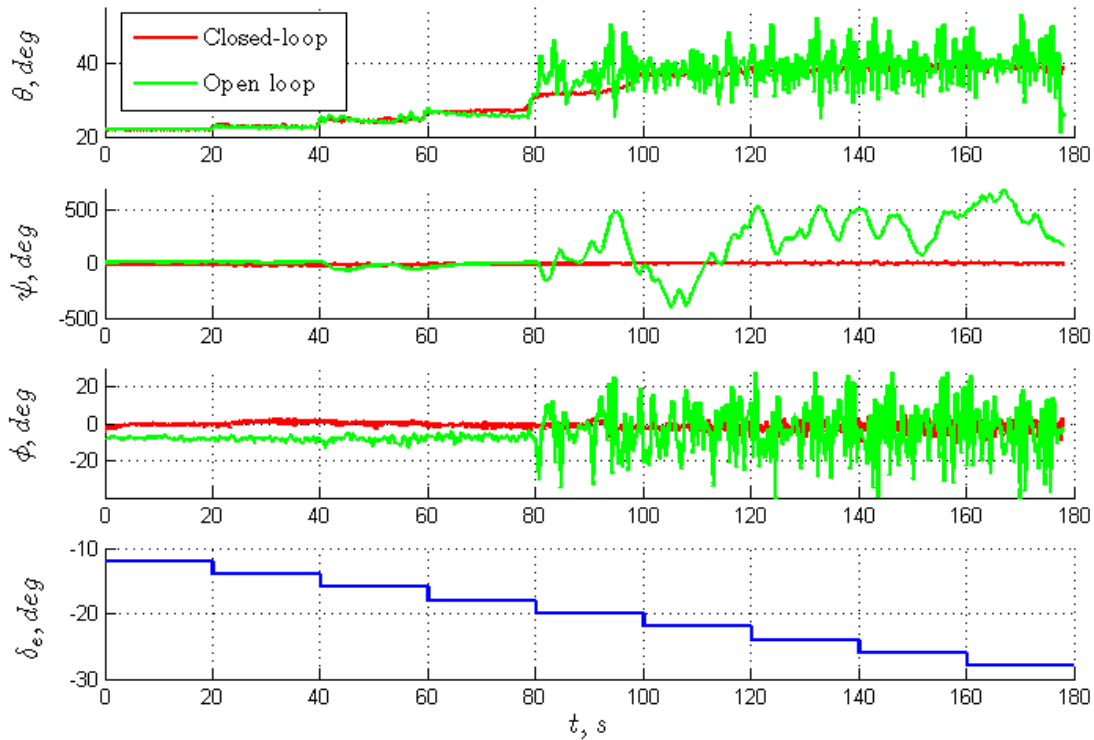

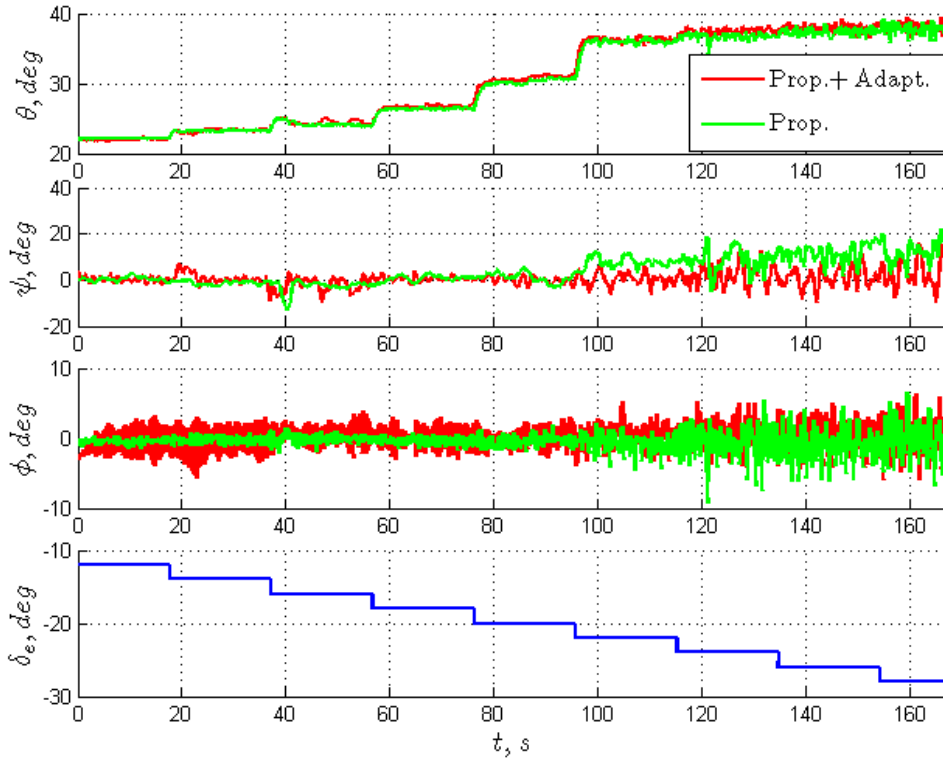Fig. 7. Open-loop and closed-loop responses.

Fig. 8. Responses of proportional and adaptive controllers.

The demonstrated results show that both controllers ensure stability in the whole available range of the model motions in 3DOF gimbals. Nevertheless, the mathematical model of motion of the mock-up mounted on 3DOF gimbals suffers from uncertainties. The conducted experiments revealed sensitivity of the designed control laws for "unspecified" perturbations. A considerable aerodynamic asymmetry at the angles of attack higher than 30 deg leads to appearance of yaw angle while using the proportional controller. Observed higher precision of the adaptive controller as compared to the proportional one can be explained by integration of the RBF weights in adaptation law (7), which enables a correction of constant uncertainties.

6 Conclusions

The technique for wind tunnel investigations of aircraft flight dynamics and control validation that uses the autonomous aircraft mock-up mounted on 3DOF gimbals is presented. Thanks to dorsal support strut oriented along the flow velocity the aircraft model can reach high angles of attack. The wind tunnel model is equipped with the on-board computer for acquisition, handling of the flight data and, simultaneously, for operation of the model control algorithms. The attitudes and rates measurements are provided by the three high resolution optical encoders and inertial measurement unit correspondingly. The mock-up has the conventional set of control surfaces driven by servos: the differential stabilator, the ailerons, and the rudder. Modelling of the autonomous flight of the wind tunnel mock-up and validation of the control laws in a semi-free flight can be carried out using the proposed technique.

Wind tunnel experiments were carried out for the dynamically scaled aircraft mock-up. In the region of the moderate angles of attack (up to $\alpha = 30$ deg) the mock-up remains stable; in the region of high angles of attack ($\alpha > 30$ deg) it loses its stability. Rotation in yaw, which is coupled with pitch and roll oscillations, is observed to be very close to dynamics of the spin motion.

The problem of stabilization of the wind tunnel model in the whole region of elevator deflection is considered. Two controllers based on the robust and MRAC techniques are designed and tested. Both control laws ensure stability in the whole available range of the model motions in 3DOF gimbals. MRAC exhibits higher accuracy of control.

References

[1] Etkin, B., *Dynamics of Atmospheric Flight*, Wiley, New York, 1972, 579 p.

[2] Ignatyev D. I., Khrabrov A.N. Neural network modeling of unsteady aerodynamic characteristics at high angles of attack. *Aerospace Science and Technology*, Vol. 41, pp. 106–115, 2015.

[3] Ignatyev D.I., Khrabrov A.N. A model of the unsteady aerodynamic characteristics at high AOA with nonlinear damping derivatives in angular rate. *Proceedings of 29th ICAS*, St.Petersburg (Russia), 2014_0449, 2014.

[4] Capone, F. J., Owens, D. B., and Hall, R. M., "Development of a Transonic Free-to-Roll Test Capability," *Journal of Aircraft*, Vol. 41, No. 3, 2004, pp. 456–463.

[5] Khrabrov, A. and Zhuk, A., Using of large amplitude free oscillations in pitch and roll to investigate unsteady aerodynamic characteristics at separated flow regimes, *Proc. of International Congress on Instrumentation in Aerospace Simulation Facilities (ICIASF'95 Record)*, Wright-Patterson AFB, OH, July 18–21, pp. 24.1–24.7, 1995.

[6] Zhuk, A. N., Stolyarov, G. I., and Khrabrov, A. N., Different modes of self-induced roll oscillations of the delta wing of small aspect ratio, *Uch. Zap. TsAGI*, vol. **24**, no. 4, pp. 113–123, 1993 (in Russian).

[7] Rajamurthy, M., "Generation of Comprehensive Longitudinal Aerodynamic Data Using Dynamic Wind-Tunnel Simulation," *Journal of Aircraft*, Vol. 34, No. 1, 1997, pp. 29–33.

[8] A. Gatto, M.H. Lowenberg, "Evaluation of a Three-Degree-of-Freedom Test Rig for Stability Derivative Estimation," *Journal of Aircraft*, Vol. 43, No. 6, 2006.

[9] S.D. Carnduff, S.D. Erbsloeh, A.K. Cooke, M.V. Cook, "Development of a low cost dynamic wind tunnel facility utilizing MEMS inertial sensors," *AIAA Aerospace Sciences Meeting and Exhibit*, Reno, Nevada, USA, AIAA Paper 2008-196, 2008.

[10] J. Pattinson, M. Lowenberg, M. Goman, "A Multi-Degree-of-Freedom Rig for the Wind Tunnel Determination of Dynamic data," *AIAA Atmospheric Flight Mechanics Conference*, Chicago, USA, 10-13 August, 2009, AIAA Paper 2009-5727.

[11] A.N. Khrabrov, M. E. Sidoryuk, E. N. Kolesnikov, Yu. A. Vinogradov, I. I. Grishin, and K. A. Kolinko, "On possibility of critical flight regime study in wind tunnels using a three-degree-of-freedom gimbals," *TsAGI Science Journal*, Vol. 45, No. 8, 2014, 825 — 839 S

[12] I. Grishin, A. Khrabrov, A. Kolinko, M. Sidoryuk, A. Vyalkov. Wind tunnel investigation of critical flight regimes using dynamically scaled actively controlled model in 3DOF gimbal. *Proceedings of 29th ICAS*, St.Petersburg (Russia), 2014_0415, 2014.

[13] D.I. Ignatyev, K.G. Zaripov, M.E. Sidoryuk, K.A. Kolinko, A.N. Khrabrov Wind Tunnel Tests for Validation of Control Algorithms at High Angles of Attack Using Autonomous Aircraft Model Mounted in 3DOF Gimbals. *AIAA Atmospheric Flight Mechanics Conference, AIAA Aviation*, Washington, D.C., USA, AIAA 2016-3106, 2016.

[14] Chilali M., Gahinet P., "H∞ design with pole placement constraints: an LMI approach," *IEEE Transactions on Automatic Control*, 41 (3) (1996) 358–367.

[15] Gahinet, P., Nemirovsky, A., Laub, A., Chilary, M. *Robust control toolbox.* The Math Works Inc., 1995

[16] Aström K. and Wittenmark B. *Adaptive Control.* 2nd edition, Addison-Weseley, Readings, 1995.

[17] Singh, S. N., Yirn, W., Wellsa, W. R., "Direct adaptive and neural control of wing-rock motion of slender delta wings," *J. of Guidance, Control, and Dynamics*, 1995, V. 18, N 1, p. 25 — 30.

[18] Calise, A. J., Shin, Y., Johnson, M. D., "A Comparison Study of Classical and Neural Network Based Adaptive Control of Wing Rock," *AIAA Guidance, Navigation, and Control Conference and Exhibit*, AIAA-

2004-5320, 16-19 August 2004, Providence, Rhode Island.

[19] Ioannou, P., Kokotovic, P., "Instability analysis and improvement of robustness of adaptive control," *Automatica*, Vol. 20, No. 5, pp. 583-594, 1984.

[20] Gorinevsky, D., "On the persistency of excitation in radial basis function network identification of nonlinear systems", *IEEE Transactions on Neural Networks*, 6 (5), 1237-1244.

7 Contact Author Email Address

mailto: d.ignatyev@mail.ru

Copyright Statement